Spatial Distributions and Interstellar Reaction Processes

Justin L. Neill,[†] Amanda L. Steber,[†] Matt T. Muckle,[†] Daniel P. Zaleski,[†] Valerio Lattanzi,[‡,§] Silvia Spezzano,[‡,§] Michael C. McCarthy,[‡,§] Anthony J. Remijan,[∥] Douglas N. Friedel,[⊥] Susanna L. Widicus Weaver,[#] and Brooks H. Pate*,[†]

[†]Department of Chemistry, University of Virginia, McCormick Road, P.O. Box 400319, Charlottesville, Virginia 22904, United States

[‡]Harvard-Smithsonian Center for Astrophysics, 60 Garden Street, Cambridge, Massachusetts 02138, United States

[§]School of Engineering and Applied Sciences, Harvard University, 29 Oxford Street, Cambridge, Massachusetts 02138, United States

[∥]National Radio Astronomy Observatory, 520 Edgemont Road, Charlottesville, Virginia 22903, United States

[⊥]Department of Astronomy, University of Illinois, Urbana, Illinois 61801, United States

[#]Department of Chemistry, Emory University, Atlanta, Georgia 30322, United States

S *Supporting Information*

ABSTRACT: Methyl formate presents a challenge for the conventional chemical mechanisms assumed to guide interstellar organic chemistry. Previous studies of potential formation pathways for methyl formate in interstellar clouds ruled out gas-phase chemistry as a major production route, and more recent chemical kinetics models indicate that it may form efficiently from radical—radical chemistry on ice surfaces. Yet, recent chemical imaging studies of methyl formate and molecules potentially related to its formation suggest that it may form through previously unexplored gas-phase chemistry. Motivated by these findings, two new gas-phase ion-molecule formation routes are proposed and characterized using electronic structure theory with conformational specificity. The proposed reactions, acid-catalyzed Fisher esterification and methyl cation transfer, both produce the less stable *trans*-conformational isomer of protonated methyl formate in relatively high abundance under the kinetically controlled conditions relevant to interstellar chemistry. Gas-phase neutral methyl formate can be produced from its protonated counterpart through either a dissociative electron recombination reaction or a proton transfer reaction to a molecule with larger proton affinity. Retention (or partial retention) of the conformation in these neutralization reactions would yield *trans*-methyl formate in an abundance that exceeds predictions under thermodynamic equilibrium at typical interstellar temperatures of ≤100 K. For this reason, this conformer may prove to be an excellent probe of gas-phase chemistry in interstellar clouds. Motivated by new theoretical predictions, the rotational spectrum of *trans*-methyl formate has been measured for the first time in the laboratory, and seven lines have now been detected in the interstellar medium using the publicly available PRIMOS survey from the NRAO Green Bank Telescope.
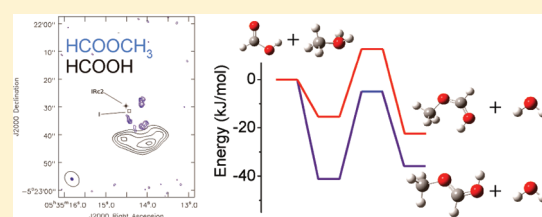
■ INTRODUCTION

Star-forming regions of our galaxy produce a rich organic and inorganic chemistry through a combination of surface and ice chemistry and gas-phase reaction processes.[1−3] Despite the low temperatures and pressures of interstellar clouds, it is possible to produce essentially the full range of organic species, including alkanes, alkenes, alkynes, arenes, alcohols, ethers, aldehydes, ketones, esters, carboxylic acids, amines, and amides.[4] Recent infrared observations[5] suggest that this organic material includes the new forms of carbon C_{60} and C_{70} that were first discovered 25 years ago in laboratory experiments designed to create the novel species produced in carbon-rich stellar outflows.[6,7] Because organic species are destroyed by high energy radiation, the organic chemistry of space occurs in molecular clouds where small carbonaceous and silicate particles, called grains, scatter high frequency radiation and shield the molecular material. These "dark" regions of the sky, where the important astronomical processes of star and planet formation occur, can only be probed by long-wavelength light, and are therefore primarily studied at frequencies below 1 THz. There are several atmospheric windows in this low-frequency region that enable ground-based telescope facilities to be used for the study of the "cool universe" through radio astronomy.

An important feature of the light collected by radio astronomical observatories is that it contains the precise signatures of molecules arising from their molecular rotational spectra. This has led to a relatively recent advance in astronomy, as the first polyatomic molecules (ammonia, water, and formaldehyde) were observed by radio astronomy just 40 years ago.[8−10] Because of the unique spectral signatures provided by rotational

spectroscopy,[11] much of the chemical inventory of the interstellar medium has been detected using radio telescopes operating in the centimeter and millimeter wavelength regions. Astronomers have routinely used single-dish telescopes, that is, large filled-aperture instruments, to search for new molecules in interstellar clouds because such searches often require the high sensitivity offered by these instruments. Observations of molecular emission from radio telescope arrays, which correlate the signals from a collection of single-dish telescopes, have been largely limited to the strongest transitions of highly abundant molecules. Despite typically having lower sensitivity compared to single-dish observations, array observations are quite useful probes of interstellar chemistry because they provide spatial information about the molecular distribution that is not readily attainable with single-dish observations. A more complete description of radio astronomical techniques as applied to the search for molecules in interstellar clouds is given in the Supporting Information.

The next-generation radio astronomy observatories, such as the Expanded Very Large Array (eVLA) and the Atacama Large Millimeter/submillimeter Array (ALMA), will provide an unprecedented view of the molecular composition of the Universe because they will incorporate both imaging capabilities and unparalleled sensitivity. A key feature of both of these observatories is broadband frequency coverage for imaging applications. For chemistry, this capability means that it will soon be possible to simultaneously obtain the spatial distribution of multiple chemical species. ALMA, in particular, will be able to generate chemical images with a higher spatial resolution than the Hubble telescope, making it possible for chemical images to become well-known in the general public as a way to see the Universe. The focus of this manuscript is to explore the potential of multispecies chemical maps to reveal mechanistic interstellar reaction chemistry through correlation of the spatial distributions of proposed reactant and product molecules.

The work presented here focuses on the synthesis of interstellar methyl formate, which has proven difficult to model by reaction kinetics networks. When only gas-phase production routes are included, the observed abundance of methyl formate is underpredicted;[12] this result has led to the introduction of surface chemistry models for the synthesis of interstellar organic species. These surface reactions mainly involve radical—radical reactions that can take place at relatively low temperatures on the ices that build up on grains.[13,14] Laboratory experiments that simulate interstellar ice chemistry show that these reactions on surfaces can contribute to methyl formate production.[15,16] Eventually, the methyl formate produced by the ice chemistry is evaporated into the gas phase by the warm-up phase associated with star formation, where this molecule and related ones can then be detected at high spectral resolution by radio astronomical observations.

It is difficult to disentangle the relative contributions of grain-surface and gas-phase chemistry to the formation of methyl formate using spectroscopic characterization alone, because such information provides only the relative abundances and temperatures of the molecules present in the cloud. It therefore remains unclear whether the current reaction network implemented in chemical models of interstellar clouds is complete, or if other chemical mechanisms that have not yet been included in these models might also contribute to methyl formate formation. Observational tests that differentiate between key grain surface and gas phase reactions could offer insight into the relative importance of these two pathways. Here we use multispecies chemical imaging of gas phase molecules to investigate whether the spatial distributions of methyl formate and related molecules are consistent with the chemistry currently included in the models and to suggest other possible chemical reaction pathways for methyl formate synthesis under interstellar conditions.

The observations that serve as a basis for this study are toward the Orion molecular cloud, which has attracted much astronomical interest due to its complex physical structure. Molecular observations play an important role in characterizing the different objects embedded in this complex environment by making it possible to visualize the outflow(s) of molecular material.[17,18] From a chemical perspective, this region is characterized by a fascinatingly rich chemical inventory as well as extreme spatial differentiation between chemical species identified though radio astronomy array measurements.[19,20] Two spatial regions have received special attention: the "Hot Core" and the "Compact Ridge." The Orion Hot Core is a warm region of molecular gas and dust, dominated by organic species containing nitrogen-based functional groups; the source of its heating is a matter of current debate.[18] The neighboring Orion Compact Ridge, meanwhile, is dominated by oxygen-containing species, including methyl formate. The work presented herein focuses on multispecies molecular distributions in this region. The spatial distributions in this region of the Orion molecular cloud have been interpreted to indicate that molecular material has been evaporated from grain surfaces by the shocks of a molecular outflow from an astronomical object with high radio continuum emission called "I," proposed to be a highly luminous young star.[17,21] The identity of this object is a topic of current interest.[18,22,23]

■ RESULTS

Chemical Images from Radio Telescope Arrays. Observations toward the Orion Kleinmann-Low (KL) region of star-formation have been obtained using two radio telescope arrays, the eVLA and the Combined Array for Research in Millimeter Astronomy (CARMA). Details of both sets of array observations, along with a more general introduction to single-dish and interferometric radio telescope facilities and a discussion of the fidelity of the images presented in this work, are given in the Supporting Information.

The spatial distributions of methyl formate and methanol determined from the eVLA observations are shown in Figure 1a. The region of highest methyl formate density is in the Orion Compact Ridge; it is slightly offset from the peak position of gas-phase methanol. The high spatial resolution mapping of methyl formate using CARMA is compared to the eVLA image in Figure 1b. This comparison shows that the morphology observed in the eVLA image is determined to a large extent by small-scale regions of methyl formate density, with the greatest density found at the position labeled MF1 (using the nomenclature of Favre et al.[24]). The type of spectral information used to create this distribution image is shown in Figure 2, where the broadband rotational spectrum at the MF1 position is shown. Several methanol transitions are present in this spectrum, from which an approximate methanol rotational temperature of 80 K is derived for this region. This temperature is similar to that reported by Favre et al.,[24] who derived an average methyl formate rotational temperature of 100 K in the MF1 region, using measurements at two different spatial resolutions. Using this information, we estimate a relative abundance ratio of methanol
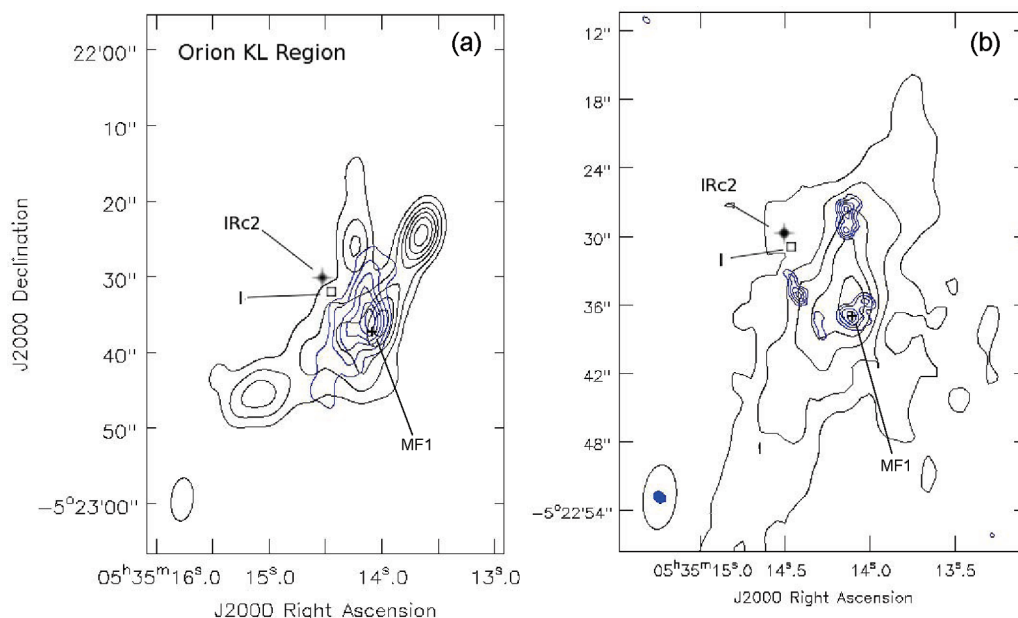
6473

dx.doi.org/10.1021/jp200539b |*J. Phys. Chem. A* 2011, 115, 6472–6480

Figure 1. (a) EVLA methyl formate (blue; contour levels = 0.12, 0.156, 0.192, 0.222, 0.252, and 0.276 Jy/beam) and methanol (black; contour levels = 11, 22, 35.75, 49.5, 66, 88, and 110 Jy/beam). (b) CARMA methyl formate (blue; contour levels = 0.2, 0.3, 0.4, 0.5, and 0.6 Jy/beam) and EVLA methyl formate (black; contour levels = 0.12, 0.156, 0.192, 0.222, 0.252, and 0.276 Jy/beam). The locations of the star IRc2, the "I" radio continuum source, and the MF1 location of methyl formate emission following the nomenclature of Favre et al.[24] are labeled. The synthesized beam widths are indicated in the lower left corner of each panel.
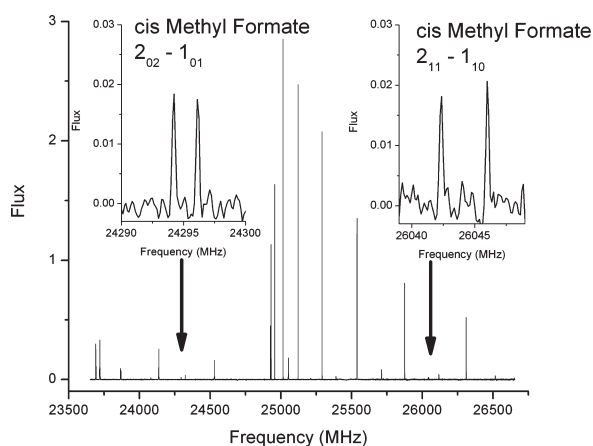

Figure 2. eVLA spectrum of the Orion molecular cloud at the position of highest methyl formate density. The strongest transitions originate from the $K = 2 \leftarrow 1$ Q-branch of methanol, while the two transitions of *cis*-methyl formate in this frequency range are shown as insets.

Table 1. Abundances of Molecules Potentially Related to Methyl Formate Production in the Orion Compact Ridge

species	$10^9 \times$ fractional abundance[a,b]
$HCOOCH_3$	30
$HCOOH$	1.4
CH_3OCH_3	19
H_2CO	40
CH_3OH	400

[a] Relative to H_2, assuming that the molecule and H_2 are coextensive. [b] Values from Sutton et al.[25]

to methyl formate in the spectrum in Figure 2 of ~15, which is roughly consistent with the abundances from Sutton et al.[25] listed in Table 1. The determination of the temperature and relative abundances of methanol and methyl formate from Figure 2 is described in detail in the Supporting Information.

Three CARMA images are shown in Figure 3. The first image, Figure 3a, compares the low spatial resolution images of formic acid and methyl formate. A simple examination of these two distributions suggests that methyl formate production near MF1 comes at the expense of formic acid, which shows an apparent decrease in its density with a morphology that complements that of methyl formate. The higher spatial resolution image of methyl formate is compared to that of formic acid in Figure 3b. The

region of highest methyl formate production is found in the area of formic acid depletion. The formic acid distribution shows no small-scale spatial regions of enhanced production in the higher spatial resolution images. The low-resolution CARMA images of dimethyl ether and methyl formate are compared in Figure 3c. There is a striking correlation between the distributions of methyl formate and dimethyl ether, suggesting that they are formed through chemically related reaction processes (that differ from formic acid production processes). The high-resolution CARMA image of dimethyl ether (not shown) indicates that the position MF1 is also the location of peak dimethyl ether formation.

Interpretation of Chemical Images Based on Chemical Reaction Processes. We propose that the spatial distributions of multiple chemical species can be used to infer chemical mechanisms that relate these molecules. A fully quantitative treatment requires that all reactions linking the various chemical species be included in the chemical reaction networks, and that spatial effects be added to the physical model through incorporation of hydrodynamics. The current state-of-the-art approaches for both of these key factors remain incomplete, limiting the interpretation of these new methyl formate observations to semiquantitative
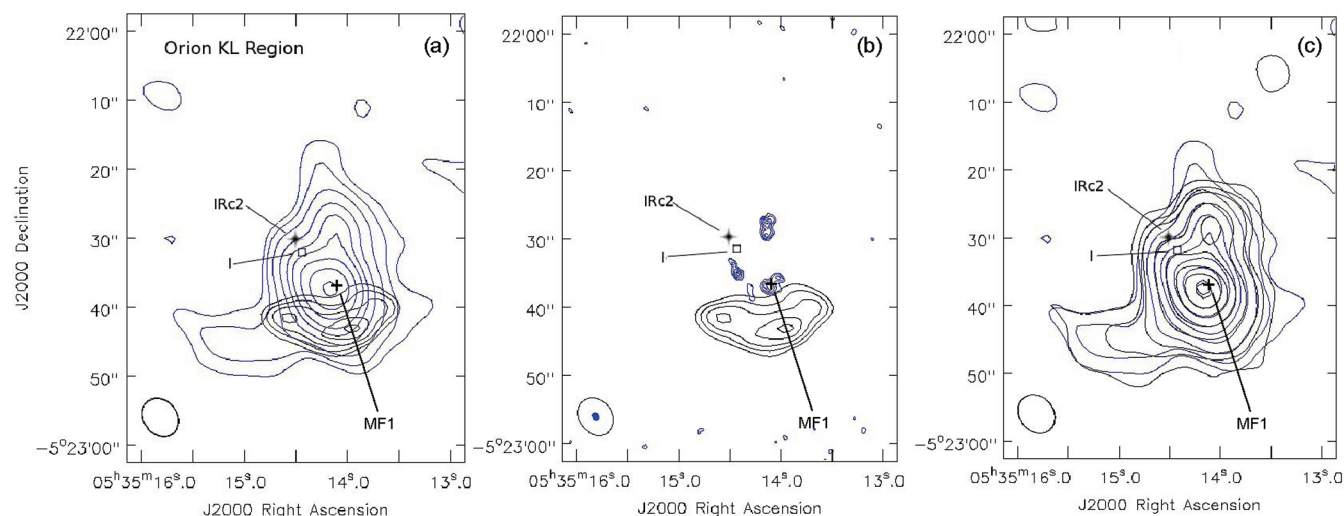
6474

dx.doi.org/10.1021/jp200539b |*J. Phys. Chem. A* 2011, 115, 6472–6480

Figure 3. (a) CARMA methyl formate (blue; contour levels = 0.08, 0.16, 0.32, 0.64, 1.04, 1.44, 2.08, 2.88, and 3.84 Jy/beam) and formic acid (black; contour levels = 0.138, 0.162, 0.186, 0.21, and 0.228 Jy/beam). (b) CARMA methyl formate (blue; contour levels = 0.2, 0.3, 0.4, 0.5, and 0.6 Jy/beam) and formic acid (black; contour levels = 0.138, 0.162, 0.186, 0.21, and 0.228 Jy/beam). (c) CARMA methyl formate (blue; contour levels = 0.08, 0.16, 0.32, 0.64, 1.04, 1.44, 2.08, 2.88, and 3.84 Jy/beam) and dimethyl ether (black; contour levels = 0.05, 0.15, 0.25, 0.65, 1.2, 1.75, 2.15, and 2.55 Jy/beam). The synthesized beam widths are indicated in the lower left corner of each panel.

results. However, it should be stressed that this work is one of the first studies to examine chemical mechanisms through spatial distributions, and as such serves as the foundation for development of a full quantitative treatment of this problem.

The addition of spatial distributions to interstellar reaction networks is a field of study in its infancy. The first report of the predicted spatial distribution of molecules for hot core chemistry indicates that the gas-phase distributions of methyl formate, formic acid, dimethyl ether, and methanol are highly correlated with a peak abundance centered on the hot core position.[26] Recent laboratory experiments of the temperature programmed desorption of organic ices shows that these four species have similar desorption temperatures.[16] Therefore, desorption from the shocks of a molecular outflow might also be expected to produce similar spatial distributions of these species. In fact, the low spatial resolution images from CARMA show that the formic acid, methyl formate, and dimethyl ether distributions have a similar large-scale distribution from east-to-west that is most clearly seen in the formic acid distribution.

As discussed above, the compact ridge region shows several deviations from this simple model. Recent gas-grain chemistry models predict that at the temperature of $\sim 80-100$ K estimated for this region, formic acid is found in an abundance equal to or greater than that of methyl formate.[13,14] However, no local enhancement of formic acid column density is observed near the MF1 position. As a result, we consider gas-phase chemical reactions that can "post-process" the organic material liberated from the grains in the Orion Compact Ridge region. Presumably, all of the material formed on grain surfaces would be deposited through the same physical mechanism (i.e., heating, shock, etc.), and therefore, the chemical products of this process would display similar spatial distributions. However, subsequent gas-phase reaction chemistry could reshape the molecular distributions and, therefore, is more likely to be revealed by studying the correlations of different molecular spatial distributions. The distributions of low-abundance species (i.e., the limiting reagents) will be most strongly affected by chemical processing.

The hypothesis that we consider here is that the spatial distributions of methyl formate and formic acid suggest that there is a gas-phase reaction process that consumes formic acid to produce methyl formate. This idea is suggested by the apparent reduction in formic acid density at the position of peak methyl formate production (MF1). We also note that this same anticorrelation of column densities is seen even more strongly in a different region of interstellar chemistry (IRAS 16293–2422), where the methyl formate density peaks in a "valley" of formic acid density.[27] (A figure showing the correlation of the spatial distributions of methyl formate and formic acid in IRAS 16293–2422 can be found in the Supporting Information.) The time scales for gas-phase processing of the material in this low-mass hot core compared to the high-mass Orion star forming region make direct comparison between the two sources difficult without a full understanding of the relative contributions of gas and grain chemical processes. However, this anticorrelation between methyl formate and formic acid emission does provide a tantalizing hint at possible reaction pathways that involve the formation of methyl formate from formic acid. Finally, the spatial distributions of methyl formate and dimethyl ether have a strong correlation, with peak production occurring near the same position. Therefore, any proposed reactions should be consistent with the close correlation between these structurally similar molecules.

Based on the proposed image interpretation, we have examined two possible methyl formate production reactions using computational chemistry. To produce significant amounts of methyl formate by gas-phase reactions, at least one of the reactants must be a high-abundance interstellar molecule. As shown in Table 1, formaldehyde and methanol are found in high abundance in the Compact Ridge region. Furthermore, ion–molecule reactions are more likely to be important under low-density conditions; protonation of the reactants can occur through proton transfer from highly abundant interstellar species such as H_3^+ and HCO^+ that have low proton affinity. One of the early proposals for interstellar methyl formate production was the reaction of protonated methanol with formaldehyde;[28,29]
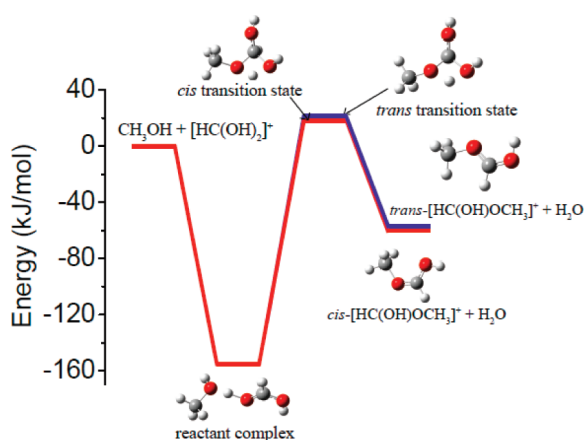
Figure 4. Energetic profile of the acid-catalyzed Fischer esterification reaction of neutral methanol and protonated formic acid, calculated at a M06-2X/6-31+G(d,p) level of theory. The energies have been corrected to account for zero-point vibrational energy. The red line corresponds to the formation of *cis*-protonated methyl formate, while the blue line corresponds to the formation of *trans*-protonated methyl formate.
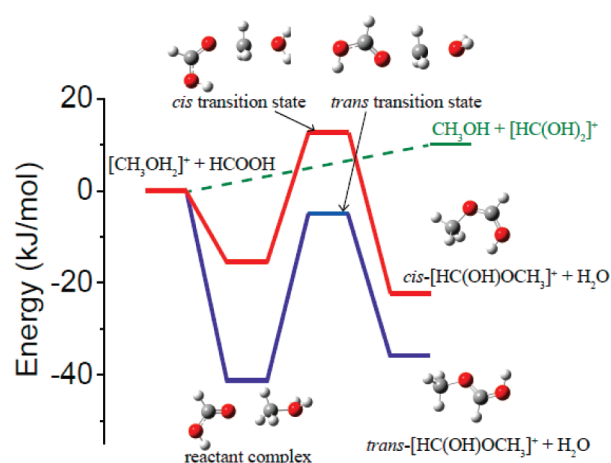

Figure 5. Energetic profile of the methyl cation transfer reaction of protonated methanol and neutral formic acid, calculated at a M06-2X/6-31+G(d,p) level of theory. The energies have been corrected to account for zero-point vibrational energy. The red line corresponds to the formation of *cis*-protonated methyl formate, while the blue line corresponds to the formation of *trans*-protonated methyl formate. The green line shows the energetics of the proton transfer reaction.

however, a computational chemistry study revealed that the barrier of this reaction is too high (128 kJ/mol) for this reaction to contribute significantly to methyl formate synthesis under interstellar conditions.[12] The ion−molecule reactions considered here involve the reaction of methanol and formic acid, where one of the reactants is protonated. These reactions were not considered in the previous computational study of the gas-phase production of methyl formate.[12]

Methyl Formate Production via Acid-Catalyzed Fischer Esterification. The reaction between neutral methanol and protonated formic acid is well-known in organic chemistry as acid-catalyzed Fischer esterification:

$$CH_3OH + [HC(OH)_2]^+ \rightarrow [HC(OH)OCH_3]^+ + H_2O \quad (1)$$
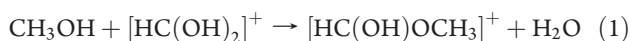
The reaction profile obtained from ab initio calculations, calculated using the Gaussian 09 software package,[30] is shown in Figure 4. In this study, we consider two approach geometries for the reactants. These different pathways have transition states that lead to different conformers of protonated methyl formate. The calculated reaction barriers are 17 and 21 kJ/mol for paths that produce *cis*- or *trans*-protonated methyl formate as products, respectively. (For comparison, the reaction barrier in the absence of acid catalysis is about 160 kJ/mol at the same level of theory.)

There are several aspects of this reaction that deserve additional comment: (1) At the temperatures estimated for the Orion Compact Ridge (∼100 K), the thermal energy (kT) is only about 1 kJ/mol, suggesting that the direct reaction by this mechanism is inefficient. It does have a stable entrance channel complex, however, and the vibrational mode with an imaginary frequency at the transition state is essentially a single hydrogen atom motion (reduced mass 1.09 u), meaning that if the complex were collisionally or radiatively stabilized,[31−33] protonated methyl formate could be formed via tunneling.[34,35] (2) This reaction also requires a large abundance of protonated formic acid, but H_3^+, which plays a central role in interstellar ion−molecule chemistry,[36−38] cannot protonate formic acid directly, as this reaction instead results in molecular dissociation.[39,40] Instead, protonation of formic acid must occur by another ion, such as

HCO^+ or H_3O^+, either of which has been shown in the laboratory to efficiently form this ion.[39−41] (3) Proton transfer between the reactants is exothermic and may be more facile; two studies found that this proton transfer pathway is the dominant reaction channel.[42,43] (4) It has also been suggested that the gas-phase esterification reaction does not proceed through the traditional Fischer mechanism, with a tetrahedral intermediate. A recent study[44] suggests that a closely related reaction, that of protonated acetic acid and methanol, may instead proceed through a proton-shuttling mechanism and might not have a reaction barrier. Due to the complexity of this pathway, the authors were unable to determine the complete reaction path; additional calculations are needed to determine whether acid-catalyzed Fischer esterification is a viable alternative mechanism to produce interstellar methyl formate.

Methyl Formate Production via Methyl Cation Transfer. The second possibility for the gas phase formation of methyl formate is the reaction between protonated methanol and neutral formic acid, a reaction previously identified by Ehrenfreund and Charnley as a possible route for interstellar methyl formate production:[3]

$$HCOOH + [CH_3OH_2]^+ \rightarrow [HC(OH)OCH_3]^+ + H_2O \quad (2)$$
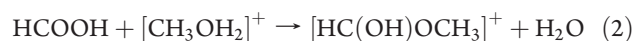
The reaction profiles for two different approach geometries are shown in Figure 5. In this reaction, a methyl cation is transferred to neutral formic acid to create protonated methyl formate and water. Gas-phase alkyl cation transfer reactions with protonated alcohols have been studied extensively in the laboratory.[45−47] For this reaction profile, we have only considered the more stable conformation of formic acid as the reactant, because the less stable conformer has not been detected in the interstellar medium. Determination of the energy of the products assumes the conformation of protonated methyl formate that is most likely to be produced based on the transition state geometry.

In contrast to the Fischer esterification reaction, calculations predict a barrierless process for the formation of protonated

methyl formate in the *trans*-conformation of the ester, while the reaction that leads to *cis*-protonated methyl formate has a barrier of about 10 kJ/mol. The reaction between formic acid and protonated methanol has been studied in the laboratory using the flowing afterglow technique at 300 K, but only products involving proton transfer between the reactants were observed.[40] This is an endothermic process[48] that is likely of little significance at typical interstellar temperatures. Unlike formic acid, methanol can be readily protonated by H_3^+; two independent experimental studies have found significant product branching ratios (∼25−30% in the low-pressure limit) for the creation of protonated methanol.[49,50] For this reason, protonated methanol is likely to be an abundant interstellar species. However, owing to the lack of rotational transition frequencies, this ion has not yet been detected in space.

It is also worth emphasizing that this reaction profile is energetically similar to that between protonated methanol and neutral methanol to produce protonated dimethyl ether; it too occurs without a barrier[51] and is considered an important contributor to interstellar dimethyl ether formation.[52] If the methyl cation transfer reaction efficiently produces methyl formate in the MF1 region, then one would expect dimethyl ether would also be produced in the same spatial region, since neutral methanol is also present in this region. The close correlation between the methyl formate and dimethyl ether molecular distributions shown in Figure 3c is consistent with a reaction chemistry linked by protonated methanol as a reagent.

Dissociation of Protonated Methyl Formate. Both reactions, but particularly the barrierless methyl cation transfer reaction, would be expected to produce significant amounts of protonated methyl formate in the less stable *trans*-conformation of the ester, but only the neutral form of methyl formate in its lower energy *cis*-conformer has been detected by radio astronomical observations. The neutral form can be produced from protonated methyl formate by dissociative electron recombination or proton transfer to a high-abundance species with higher proton affinity.

Dissociative recombination reactions of several organic ions of interstellar interest have been studied in recent years using the heavy ion storage ring CRYRING.[53−57] These studies find that molecular fragmentation is a major product channel owing to the large exothermicity for this type of neutralization reaction. However, chemical kinetics models recently calculated that the gas-phase synthesis of dimethyl ether through its protonated counterpart could produce the observed abundance of dimethyl ether in the interstellar medium, even assuming a low branching fraction for the production of neutral dimethyl ether.[13] Despite the apparent inefficiency of the dissociative recombination process, ion−molecule synthetic routes still have great significance in interstellar chemistry.

Although a study of methyl formate dissociative recombination has not been published, a recent study of structurally similar formic acid has been reported.[57] This study found that 13% of reactions did not result in any heavy atom bond breaking. The exact composition of the remaining 87% could not be quantitatively determined, but energetically, the two most favorable processes are molecular dissociations leading to $CO_2 + H_2$ and $CO + H_2O$, with barriers of ∼290 kJ/mol;[58] bond cleavage, alternatively, to form $HCO + OH$, requires ∼450 kJ/mol of energy.[59] Methyl formate can dissociate with qualitatively similar barriers.[60,61] Because of its higher proton affinity, additionally, the methyl formate dissociative recombination reaction is less
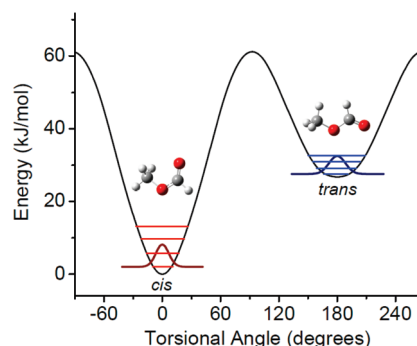

Figure 6. Potential of conformational isomerization of methyl formate, calculated at a MP2/6-31++G(d,p) level of theory. The red and blue lines represent the first four torsional energy levels of each conformer.

exothermic than that of formic acid,[62] so it is possible that the formation of neutral methyl formate could have a higher branching ratio than in the corresponding formic acid reaction.

There is also the possibility that the conformational specificity of the proposed reactions could be degraded in the conversion to neutral methyl formate. Nevertheless, we propose that if these ion−molecule reactions make a meaningful contribution to the total production of gas-phase interstellar methyl formate, then it is likely that the less stable *trans*-conformer of neutral methyl formate would be produced in a high enough abundance for its radio astronomical detection. The ab initio conformational potential of neutral methyl formate is shown in Figure 6. Our calculations agree with those of Senent et al.[63] The *trans*-conformer is less stable than *cis*-methyl formate by about 25 kJ/mol, with the difference in conformer stability arising from electrostatic effects rather than a steric interaction.[64,65] The conformational potential energy surface of methyl formate is very similar to that of formic acid.[58,66,67] Under thermodynamic equilibrium at 100 K, the abundance of the *trans*-conformer is about 10^{-14} of that of the *cis*-conformer, which would make the *trans*-conformer undetectable by radio astronomy. Because the barrier for the interconversion from *trans* to *cis* is calculated to be ∼35 kJ/mol, it is probable that any neutral *trans*-methyl formate produced will remain in this conformation under interstellar conditions. If the *trans*-conformer of neutral methyl formate could be detected by radio astronomy, it may provide strong, albeit circumstantial, evidence for gas-phase, ion−molecule reactions that contribute significantly to interstellar methyl formate production.

Interstellar Detection of the Less Stable Conformer of Methyl Formate. Because the rotational spectrum of *trans*-methyl formate has not been previously reported, its spectrum has been sought experimentally. Here molecular beam conditions were employed using chirped-pulse Fourier transform microwave (FTMW) spectroscopy[68] in the 6.5−18.5 and 25−40 GHz regions, and microwave−microwave double-resonance spectroscopy in a cavity FTMW spectrometer. The population of the less stable conformer in the pulsed jet expansion was increased significantly using a pulsed discharge nozzle source.[69] This source increased the signal levels of the *trans*-conformation by a factor of ∼30, making possible the double-resonance spectroscopy measurements that were used to confirm the assignments. The double-resonance measurements were needed because the *trans*-conformer has a low barrier to methyl group internal rotation that leads to an unusual, but interpretable, pattern of the rotational transitions in each of the two torsional

Table 2. Structural Parameters Obtained from Analysis of the Pure Rotational Spectrum of *trans*-Methyl Formate and from Electronic Structure Calculations

parameter	experiment	ab initio[a]
A (MHz)	47426 (3)	47138
B (MHz)	4747.59 (11)	4693
C (MHz)	4398.490 (4)	4390
V_3 (cm^{-1})[b]	12.956 (17)	22.6
ρ (unitless)	0.27347 (3)	0.266

[a] Gaussian 09;[30] MP2/6-311++G(d,p). [b] The last two parameters are related to the methyl internal rotation and are the barrier to internal rotation and the internal rotation—overall rotation coupling constant,

$$\rho = I_\alpha \sqrt{\frac{\lambda_a^2}{l_a^2} + \frac{\lambda_b^2}{l_b^2}}$$

where λ_a and λ_b are the direction cosines between the methyl internal rotor axis and the a and b principal axes and I_α is the moment of inertia of the methyl top. These parameters are obtained by fitting the experimental spectrum to the rho-axis method Hamiltonian using the BELGI analysis program.[70,71]

Table 3. Laboratory Measured Pure Rotational Transition Frequencies of *trans*-Methyl Formate Observed in Sgr B2(N)

J'	K_a'	K_c'	J''	K_a''	K_c''	ν_A (MHz)	ν_E (MHz)	$\nu_E - \nu_A$ (MHz)
1	0	1	0	0	0	9124.2209	9207.4274	83.2065
2	0	2	1	0	1	18247.0384	18367.8481	120.8097
3	0	3	2	0	2	27367.0480	27440.9922	73.9442

tunneling ground states. The full details of the experiment and the interpretation of the rotational spectrum will be presented in a separate publication. Table 2 presents experimental values of several structural parameters for the molecule, fit to the rho-axis Hamiltonian using the BELGI program.[70,71] The agreement between the experimental parameters and the parameters calculated using computational chemistry confirm the assignment that *trans*-methyl formate is the carrier of the observed lines.

The measured rotational transition frequencies for the strongest *a*-type rotational transitions between 8 and 28 GHz are reported in Table 3. In Figure 7 we show the detection of these transitions in the publically available PRIMOS survey spectrum measured by the NRAO Green Bank Telescope.[72] We want to emphasize that this survey is of the Sagittarius molecular cloud (Sgr B2(N)) and not the Orion molecular cloud, the source of the chemical images that were the original motivation for this work. The PRIMOS survey was used because it is presently the only available survey that covers the spectral range where we have obtained laboratory rotational transition frequencies for the *trans*-conformer. Nevertheless, we have established that the less stable conformation of methyl formate can be produced by reactions that are feasible under interstellar conditions.

◼ DISCUSSION

The fundamental premise of this work is that the interstellar spatial distributions of chemically related species are influenced by the reaction chemistry and, therefore, convey information about the chemical production route; however, we acknowledge that astrophysical effects might also lead to the observed correlations (and anticorrelations). Modeling studies have shown that
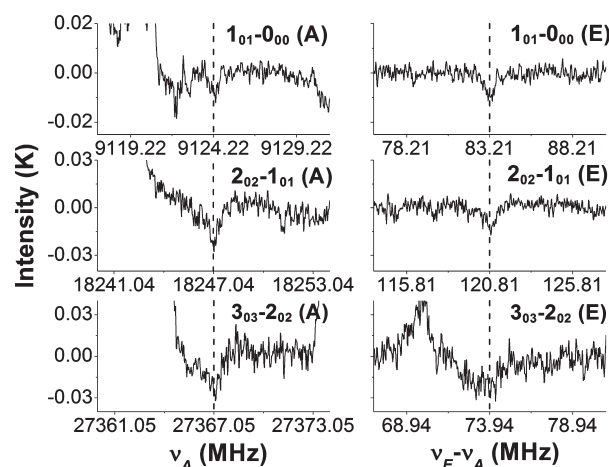

Figure 7. Transitions of *trans*-methyl formate detected in Sgr B2(N) by the Green Bank Telescope. The frequencies have been Doppler shifted to +64 km/s, the systematic velocity of this source. The dashed lines indicate the laboratory transition frequencies.

observed molecular abundances are highly dependent on the temperature and warm-up time scale.[13,14,73] Examination of the temperature-dependent results from Laas et al.[73] show that methyl formate is formed efficiently on grain surfaces in the range of 30—70 K. At temperatures greater than 50 K, the methyl formate gas-phase abundance begins to increase as a result of its evaporation from the ice. The grain-surface and gas-phase abundances of formic acid are markedly different from those of methyl formate in the same temperature range, remaining essentially constant in both cases. It is only at higher temperatures ($T > 90$ K, that is, where the water ice matrix begins to evaporate) that the gas-phase formic acid abundance begins to increase. It is possible, then, for methyl formate to be liberated from ice mantles and formic acid to still be trapped in the water ice matrix in regions where the local temperature is in the range of 70—90 K. The gas-phase methyl formate abundance would peak in these slightly colder regions, whereas the formic acid abundance would peak in warmer regions.

In addition to the more general case of temperature differentiation, a mechanism allowing for the sudden release of ice mantles (i.e., shocks) would lock the gas-phase abundances into the relative ratios dictated by the grain surface chemistry at the temperature of the event. The spatial distribution of formic acid in the Orion Compact Ridge has been interpreted to represent a shock boundary, as a number of water masers can be found near the region of highest formic acid abundance.[74] The observed gas-phase organic material would have been liberated from grains in the preshock region south of MF1. In Figure 3 it can be seen that, in this region, indeed, methyl formate, dimethyl ether, and formic acid display similar spatial distributions. The new gas-phase reactions proposed in this paper are based on molecular abundances in the MF1 region, where formic acid is present at a far lower abundance than methyl formate or dimethyl ether. This region could be one that is shielded from the outflow, or one where postshock chemistry has occurred. Regardless of the delivery mechanism for the gas-phase material, it is quite likely that this material will be additionally processed in regions where the time scales are sufficiently long for gas-phase reactions to occur. Further molecular spatial mapping of other interstellar environments with higher image fidelity in the coming years will

help to clarify the role of chemical and astrophysical effects in shaping molecular spatial distributions.

Using available interstellar radio astronomical surveys, we have been able to show that the less stable conformer of trans methyl formate is produced in the Sgr B2(N) region. A specific weakness of this new molecular identification in terms of our chemical arguments is that the spatial images that led to the proposal of detectable amounts of *trans*-methyl formate were obtained in a different interstellar location, the Orion region. The identification of this conformer does not prove that the proposed reactions are responsible for its presence, but this is a common limitation of physical organic chemistry arguments. The gas-phase reactions proposed here have been added to existing interstellar reaction networks; a recent modeling study which includes these reactions found that *trans*-methyl formate can be produced at a detectable abundance by the gas-phase methyl cation transfer reaction.[73] Future laboratory and radio astronomical observations are needed to further test these reactions. In addition to observations focused on detecting *trans*-methyl formate in the Orion Compact Ridge, the protonated forms of methanol, dimethyl ether, and methyl formate are new targets for laboratory rotational spectroscopy, as they might be present at sufficiently high column densities to enable detection if these proposed reactions are indeed important in these environments.

CONCLUSIONS

Multispecies chemical images of chemically rich regions of the interstellar medium have been used to examine the production of methyl formate in the Compact Ridge region of the Orion molecular cloud. The correlation of the column density profiles of low abundance species was used to suggest the reaction partners in the chemical reaction. The chemical images in Orion and another interstellar region, IRAS 16293-2422, suggest the gas-phase conversion of formic acid to methyl formate. Two possible ion—molecule reactions between formic acid and methanol investigated by computational chemistry are suggested to be viable interstellar reaction routes. The conformer specific reaction paths suggest that these reactions could lead to a relatively high abundance of the less stable *trans*-conformer of methyl formate under the kinetically controlled conditions expected to hold in interstellar reaction environments. Based on the proposed reactions, the laboratory identification of the less stable conformation of methyl formate has been made using rotational spectroscopy. This conformer is detected in the publicly available PRIMOS survey spectrum from the Green Bank Telescope of a different chemically rich interstellar region (Sgr B2(N)).

This work suggests that the coming availability of high spatial resolution chemical images from next-generation radio astronomical observatories will provide a new way to explore mechanistic interstellar chemistry. The unusual chemical environments in the interstellar medium can produce novel chemical reaction processes that complement the synthesis techniques common under terrestrial conditions with the potential to generate new types of chemical species and materials. This chemistry may also play a key role in providing the basic chemical materials to newly forming planetary systems that can, under favorable conditions, possibly develop life. A better understanding of the chemical reaction processes at work in different interstellar environments can also be used to advance our understanding of formation of important astronomical objects, including stars and planets. The development of analysis methods to interpret multispecies

chemical images from radio astronomy has the potential to make chemistry a fundamental tool for exploring the structure and evolution of the Universe.

ASSOCIATED CONTENT

S **Supporting Information.** Details of the eVLA and CARMA observations; Figure S1 with transitions of *trans*-methyl formate observed by the GBT on a velocity scale; Figure S2 showing the spatial distributions of methyl formate and formic acid in IRAS 16293-2422 from ref 27; details of the temperature derivation of methanol and the relative abundances of methanol and methyl formate from Figure 2. This material is available free of charge via the Internet at http://pubs.acs.org.

AUTHOR INFORMATION

Corresponding Author
*E-mail: brookspate@virginia.edu.

ACKNOWLEDGMENT

REFERENCES

(1) Herbst, E.; van Dishoeck, E. F. *Annu. Rev. Astron. Astrophys.* **2009**, *47*, 427–480.

(2) van Dischoek, E. F.; Blake, G. A. *Annu. Rev. Astron. Astrophys.* **1998**, *36*, 317–368.

(3) Ehrenfreund, P.; Charnley, S. B. *Annu. Rev. Astron. Astrophys.* **2000**, *38*, 427–483.

(4) Woon, D. *The Astrochymist*. http://www.astrochymist.org/.

(5) Cami, J.; Bernard-Salas, J.; Peeters, E.; Malek, S. E. *Science* **2010**, *329*, 1180–1182.

(6) Kroto, H. W.; Heath, J. R.; O'Brien, S. C.; Curl, R. F.; Smalley, R. E. *Nature* **1985**, *318*, 162–163.

(7) Kroto, H. W. *Philos. Trans. R. Soc., A* **1988**, *325*, 405–421.

(8) Cheung, A. C.; Rank, D. M.; Townes, C. H.; Thornton, D. D.; Welch, W. J. *Phys. Rev. Lett.* **1968**, *21*, 1701–1705.

(9) Cheung, A. C.; Rank, D. M.; Townes, C. H.; Thornton, D. D.; Welch, W. J. *Nature* **1969**, *221*, 626–628.

(10) Snyder, L. E.; Buhl, D.; Zuckerman, B.; Palmer, P. *Phys. Rev. Lett.* **1969**, *22*, 679–681.

(11) Gordy, W.; Cook, R. L. *Microwave Molecular Spectra*; John Wiley and Sons: New York, 1984.

(12) Horn, A.; Møllendal, H.; Sekiguchi, O.; Uggerud, E.; Roberts, H.; Herbst, E.; Viggiano, A. A.; Fridgen, T. D. *Astrophys. J.* **2004**, *611*, 605–614.

(13) Garrod, R. T.; Herbst, E. *Astron. Astrophys.* **2006**, *457*, 927–936.

(14) Garrod, R. T.; Widicus Weaver, S. L.; Herbst, E. *Astrophys. J.* **2008**, *682*, 283–302.

(15) Bennett, C. J.; Kaiser, R. I. *Astrophys. J.* **2007**, *661*, 899–909.

(16) Öberg, K. I.; Garrod, R. T.; van Dishoeck, E. F.; Linnartz, H. *Astron. Astrophys.* **2009**, *504*, 891–913.

(17) Blake, G. A.; Mundy, L. G.; Carlstrom, J. E.; Padin, S.; Scott, S. L.; Scoville, N. Z.; Woody, D. P. *Astrophys. J.* **1996**, *472*, L49–L52.

(18) Zapata, L. A.; Schmid-Burgk, J.; Menten, K. M. *Astron. Astrophys.* **2010**, *529*, A24.

(19) Guélin, M.; Brouillet, N.; Cernicharo, J.; Combes, F.; Wooten, A. *Astrophys. Space Sci.* **2008**, *313*, 45–51.

(20) Friedel, D. N.; Snyder, L. E. *Astrophys. J.* **2008**, *672*, 962–973.

(21) Menten, K. M.; Reid, M. J. *Astrophys. J.* **1995**, *445*, L157–160.

(22) Plambeck, R. L.; Wright, M. C. H.; Friedel, D. N.; Widicus Weaver, S. L.; Bolatto, A. D.; Pound, M. W.; Woody, D. P.; Lamb, J. W.; Scott, S. L. *Astrophys. J.* **2009**, *704*, L25–L28.

(23) Reid, M. J.; Menten, K. M.; Greenhill, L. J.; Chandler, C. J. *Astrophys. J.* **2007**, *664*, 950–955.

(24) Favre, C.; Despois, D.; Brouillet, N.; Baudry, A.; Combes, F.; Guélin, M.; Wootten, A.; Wlodarczak, G. *Astron. Astrophys.* **2011**, arXiv:1103.2548v1.

(25) Sutton, E. C.; Peng, R.; Danchi, W. C.; Jaminet, P. A.; Sandell, G.; Russell, A. P. G. *Astrophys. J., Suppl. Ser.* **1995**, *97*, 455–496.

(26) Aikawa, Y.; Wakelam, V.; Garrod, R. T.; Herbst, E. *Astrophys. J.* **2008**, *674*, 993–1005.

(27) Remijan, A. J.; Hollis, J. M. *Astrophys. J.* **2006**, *640*, 842–848.

(28) Blake, G. A.; Sutton, E. C.; Masson, C. R.; Phillips, T. G. *Astrophys. J.* **1987**, *315*, 621–645.

(29) Millar, T. J.; Herbst, E.; Charnley, S. B. *Astrophys. J.* **1991**, *369*, 147–156.

(30) Frisch, M. J.; Trucks, G. W.; Schlegel, H. B.; Scuseria, G. E.; Robb, M. A.; Cheeseman, J. R.; Scalmani, G.; Barone, V.; Mennucci, B.; Petersson, G. A.; Nakatsuji, H.; Caricato, M.; Li, X.; Hratchian, H. P.; Izmaylov, A. F.; Bloino, J.; Zheng, G.; Sonnenberg, J. L.; Hada, M.; Ehara, M.; Toyota, K.; Fukuda, R.; Hasegawa, J.; Ishida, M.; Nakajima, T.; Honda, Y.; Kitao, O.; Nakai, H.; Vreven, T.; Montgomery, J. A., Jr.; Peralta, J. E.; Ogliaro, F.; Bearpark, M.; Heyd, J. J.; Brothers, E.; Kudin, K. N.; Staroverov, V. N.; Kobayashi, R.; Normand, J.; Raghavachari, K.; Rendell, A.; Burant, J. C.; Iyengar, S. S.; Tomasi, J.; Cossi, M.; Rega, N.; Millam, J. M.; Klene, M.; Knox, J. E.; Cross, J. B.; Bakken, V.; Adamo, C.; Jaramillo, J.; Gomperts, R.; Stratmann, R. E.; Yazyev, O.; Austin, A. J.; Cammi, R.; Pomelli, C.; Ochterski, J. W.; Martin, R. L.; Morokuma, K.; Zakrzewski, V. G.; Voth, G. A.; Salvador, P.; Dannenberg, J. J.; Dapprich, S.; Daniels, A. D.; Farkas, O.; Foresman, J. B.; Ortiz, J. V.; Cioslowski, J.; Fox, D. J. *Gaussian 09*; Gaussian, Inc.: Wallingford, CT, 2009.

(31) Thölmann, D.; McCormick, A.; McMahon, T. B. *J. Phys. Chem.* **1994**, *98*, 1156–1160.

(32) Fridgen, T. D.; McMahon, T. B. *J. Phys. Chem. A* **2001**, *105*, 1011–1019.

(33) Ryzhov, V.; Yang, Y.-C.; Klippenstein, S. J.; Dunbar, R. C. *J. Phys. Chem. A* **1998**, *102*, 8865–8870.

(34) Herbst, E.; DeFrees, D. J.; Talbi, D.; Pauzat, F.; Koch, W.; McLean, A. D. *J. Chem. Phys.* **1991**, *94*, 7842–7849.

(35) Herbst, E.; Yamashita, K. *J. Chem. Soc., Faraday Trans* **1993**, *89*, 2175–2183.

(36) McCall, B. J.; Oka, T. *Science* **2000**, *287*, 1941–1942.

(37) Watson, W. D. *Astrophys. J.* **1973**, *183*, L17–L20.

(38) Herbst, E.; Klemperer, W. *Astrophys. J.* **1973**, *185*, 505–533.

(39) Mackay, G. I.; Hopkinson, A. C.; Bohme, D. K. *J. Am. Chem. Soc.* **1978**, *100*, 7460–7464.

(40) Freeman, C. G.; Harland, P. W.; McEwan, M. J. *Aust. J. Chem.* **1978**, *31*, 2157–2160.

(41) Mackay, G. I.; Tanner, S. D.; Hopkinson, A. C.; Bohme, D. K. *Can. J. Chem.* **1979**, *57*, 1518–1523.

(42) Feng, W. Y.; Lifshitz, C. *J. Phys. Chem.* **1994**, *98*, 3658–3663.

(43) Tiedemann, P. W.; Riveros, J. M. *J. Am. Chem. Soc.* **1974**, *96*, 185–189.

(44) Fileti, E. E.; de Oliveira, A. E.; Morgon, N. H.; Riveros, J. M. *Int. J. Quantum Chem.* **2011**, *111*, 1596–1606.

(45) Moet-Ner, M.; Karpas, Z. *J. Phys. Chem.* **1986**, *90*, 2206–2210.

(46) Karpas, Z.; Moet-Ner, M. *J. Phys. Chem.* **1989**, *93*, 1859–1863.

(47) Fridgen, T. D.; Keller, J. D.; McMahon, T. B. *J. Phys. Chem. A* **2001**, *105*, 3816–3824.

(48) Freeman, C. G.; Harland, P. W.; McEwan, M. J. *Int. J. Mass Spectrom. Ion Phys.* **1978**, *28*, 377–388.

(49) Huntress, W. T.; Bowers, M. T. *Int. J. Mass Spectrom. Ion Phys.* **1973**, *12*, 1–18.

(50) Fiaux, A.; Smith, D. L.; Futrell, J. H. *Int. J. Mass Spectrom. Ion Phys.* **1976**, *20*, 223–235.

(51) Bouchoux, G.; Choret, N. *Rapid Commun. Mass Spectrom.* **1997**, *11*, 1799–1807.

(52) Peeters, Z.; Rodgers, S. D.; Charnley, S. B.; Schriver-Mazzouli, L.; Schriver, A.; Keane, J. V.; Ehrenfreund, P. *Astron. Astrophys.* **2006**, *445*, 197–204.

(53) Neau, A.; Khalili, A.Al; Rosen, S.; Le Padellec, A.; Derkatch, A. M.; Shi, W.; Vikor, L.; Larsson, M.; Semaniak, J.; Thomas, R.; Nagard, M. B.; Andersson, K.; Danared, H.; af Ugglas, M. *J. Chem. Phys.* **2000**, *113*, 1762–1770.

(54) Geppert, W. D.; Hamberg, M.; Thomas, R. D.; Österdahl, F.; Hellberg, F.; Zhaunerchyk, V.; Ehlerding, A.; Millar, T. J.; Roberts, H.; Semaniak, J.; af Ugglas, M.; Källberg, A.; Simonsson, A.; Kaminska, M.; Larsson, M. *Faraday Discuss* **2006**, *133*, 177–190.

(55) Hamberg, M.; Geppert, W. D.; Thomas, R. D.; Zhaunerchyk, V.; Österdahl, F.; Ehlerding, A.; Kaminska, M.; Semaniak, J.; af Ugglas, M.; Källberg, A.; Paal, A.; Simonsson, A.; Larsson, M. *Mol. Phys.* **2007**, *105*, 899–906.

(56) Hamberg, M.; Österdahl, F.; Thomas, R. D.; Zhaunerchyk, V.; Vigren, E.; Kaminska, M.; af Ugglas, M.; Källberg, A.; Simonsson, A.; Paál, A.; Larsson, A.; Geppert, W. D. *Astron. Astrophys.* **2010**, *514*, A83.

(57) Vigren, E.; Hamberg, M.; Zhaunerchyk, V.; Kaminska, M.; Semaniak, J.; Larsson, M.; Thomas, R. D.; af Ugglas, M.; Kashperka, I.; Millar, T. J.; Walsh, C.; Roberts, H.; Geppert, W. D. *Astrophys. J.* **2010**, *709*, 1429–1434.

(58) Goddard, J. D.; Yamaguchi, Y.; Schaefer, H. F., III *J. Chem. Phys.* **1992**, *96*, 1158–1166.

(59) Glockler, G. *J. Phys. Chem.* **1959**, *63*, 828–832.

(60) Francisco, J. S. *J. Am. Chem. Soc.* **2003**, *125*, 10475–10480.

(61) Metcalfe, W. K.; Simmie, J. M.; Curran, H. J. *J. Phys. Chem. A* **2010**, *114*, 5478–5484.

(62) Hunter, E. P. L.; Lias, S. G. *J. Phys. Chem. Ref. Data* **1998**, *27*, 413–656.

(63) Senent, M. L.; Villa, M.; Meléndez, F. J.; Dominguez-Gómez, R. *Astrophys. J.* **2005**, *627*, 567–576.

(64) Wennerström, H.; Forsén, S.; Roos, B. *J. Phys. Chem.* **1972**, *76*, 2430–2436.

(65) Fausto, R.; Teixeira-Dias, J. J. C. *J. Mol. Struct.* **1987**, *150*, 381–389.

(66) Wiberg, K. B.; Laidig, K. E. *J. Am. Chem. Soc.* **1987**, *109*, 5935–5943.

(67) Peterson, M. R.; Csizmadia, I. G. *J. Am. Chem. Soc.* **1979**, *101*, 1076–1079.

(68) Brown, G. G.; Dian, B. C.; Douglass, K. O.; Geyer, S. M.; Shipman, S. T.; Pate, B. H. *Rev. Sci. Instrum.* **2008**, *79*, 053103.

(69) McCarthy, M. C.; Chen, W.; Travers, M. J.; Thaddeus, P. *Astrophys. J. Suppl. Ser.* **2000**, *129*, 611–623.

(70) Hougen, J. T.; Kleiner, I.; Godefroid, M. *J. Mol. Spectrosc.* **1994**, *163*, 559–586.

(71) Kisiel, Z. *PROSPE - Programs for ROtational SPEctroscopy.* http://www.ifpan.edu.pl/~kisiel/prospe.htm.

(72) Hollis, J. M.; Remijan, A. J.; Jewell, P. R.; Lovas, F. J. *The GBT PRIMOS Project.* http://www.cv.nrao.edu/~aremijan/PRIMOS.

(73) Laas, J; Garrod, R. T.; Herbst, E.; Widicus Weaver, S. L. *Astrophys. J.* **2011**, *728*, 71.

(74) Liu, S.-Y.; Girart, J. M.; Remijan, A. J.; Snyder, L. E. *Astophys. J.* **2002**, *576*, 255–263.

6480

dx.doi.org/10.1021/jp200539b |*J. Phys. Chem. A* 2011, 115, 6472–6480